2005

Structural analysis of ferromagnetic Mn-doped ZnO thin films deposited by radio frequency magnetron sputtering

C. Liu
Virginia Commonwealth University, cliu@vcu.edu

F. Yun
Virginia Commonwealth University

B. Xiao
Virginia Commonwealth University

See next page for additional authors

Liu, C., Yun, F., Xiao, B., et al. Structural analysis of ferromagnetic Mn-doped ZnO thin films deposited by radio frequency magnetron sputtering. Journal of Applied Physics 97, 126107 (2005). Copyright © 2005 AIP Publishing LLC.

Structural analysis of ferromagnetic Mn-doped ZnO thin films deposited by radio frequency magnetron sputtering

C. Liu,[a] F. Yun, B. Xiao, S.-J. Cho, Y. T. Moon, and H. Morkoç
Department of Electrical Engineering, Virginia Commonwealth University, Richmond, Virginia 23284

Morad Abouzaid and R. Ruterana
Structure des Interfaces et Fonctionnalité des Couches Minces (SIFCOM) Unite Mixte de Recherche (UMR) 6176 Centre National de la Recherche Scientifique (CNRS)-Ecole Nationale Supérieure d'Ingénieurs de Caen (ENSICAEN), 6, Boulevard du Marechal Juin, 14050 Caen Cedex, France

K. M. Yu and W. Walukiewicz
Lawrence Berkeley National Laboratory, Berkeley, California 94720

(Received 16 December 2004; accepted 4 May 2005; published online 29 June 2005)

We report on the structural analysis of ferromagnetic Mn-doped ZnO thin films deposited by radio frequency magnetron sputtering, using transmission electron microscopy (TEM), high-resolution x-ray diffraction, and Rutherford backscattering spectroscopy (RBS) measurements. The ferromagnetic Mn-doped ZnO film showed magnetization hysteresis at 5 and 300 K. A TEM analysis revealed that the Mn-doped ZnO included a high density of round-shaped cubic and elongated hexagonal MnZn oxide precipitates. The incorporation of Mn caused a large amount of structural disorder in the crystalline columnar ZnO lattice, although the wurtzite crystal structure was maintained. The observed ferromagnetism is discussed based on the structural characteristics indicated by TEM and the behavior of Mn when it is substituted into a ZnO lattice derived from RBS measurements. © *2005 American Institute of Physics*. [DOI: 10.1063/1.1941465]

Transition-metal-doped ZnO has attracted the attention of researchers as a promising diluted magnetic semiconductor (DMS) material for its use in spintronics. DMS is a type of semiconductor in which magnetic transition-metal ions replace a fraction of cations of the host semiconductor material.[1] Based on the prediction of Dietl *et al.*,[2] considerable effort has been focused on achieving reliable ZnO-based DMS with a Curie temperature well above room temperature by doping with transition metals, especially Mn and Co.[3–7] Ferromagnetism was recently observed in insulating (Zn,Mn)O,[3] *n*-type (Zn,Mn)O,[4] and *p*-type (Zn,Mn)O.[5] However, the absence of ferromagnetic ordering in (Zn,Mn)O was also reported.[6,7]It is understood that there is a great deal of controversy in the magnetic properties of (Zn,Mn)O reported by different research groups, and it is crucial to carefully investigate the underlying mechanism of the observed magnetic properties. To develop a better understanding of the observed magnetic behavior, a microstructural analysis of transition-metal-doped ZnO thin films will be essential because the incorporation of transition metals may lead to structural disorder or the formation of transition-metal-related microclusters in the films.[8–10] The existence of such type of structural imperfections can impede the clarification of experimentally observed ferromagnetism in DMS materials. In this paper, we report on the structural analysis of ferromagnetic Mn-doped ZnO thin films deposited by radio frequency (rf) magnetron sputtering using transmission electron microscopy (TEM), x-ray diffraction (XRD), and Rutherford backscattering spectroscopy (RBS).

[a]Author to whom correspondence should be addressed; electronic mail: cliu@vcu.edu

As confirmed by TEM, a 0.35-μm-thick Mn-doped ZnO thin film was deposited on a 0.15-μm-thick undoped ZnO buffer layer using a *c*-plane sapphire substrate by the rf magnetron cosputtering of ZnO and Mn targets in an Ar gas ambient. The ZnO buffer layer and the Mn-doped ZnO film were deposited at 650 and 550 °C, respectively. A rf power of 150 W was used to sputter the ZnO target. The dc power applied to the Mn target was 5 W for the Mn-doped ZnO film. The as-deposited film was annealed at 850 °C for 1 h in air to improve the crystalline quality. The Mn content of the Mn-doped ZnO film was estimated by RBS. The crystallographic properties of the thin film were investigated by high-resolution XRD using a Cu K_α source (Philips, X'Pert). The microstructure of the Mn-doped ZnO film was examined by TEM. The magnetic properties of the Mn-doped ZnO film were determined using a commercial superconducting quantum interference device (SQUID) magnetometer (Quantum Design, MPMS).

Figure 1 shows the field-dependent magnetization curves of a $Zn_{1-x}Mn_xO$ ($x=0.07$) film at 5 and 300 K. Hysteresis loop behavior is observed at both temperatures although the magnetization at 300 K is relatively weak. The magnetic signal from the sapphire substrate was subtracted in these measurements. Temperature-dependent magnetization (M vs T) measurements of the Mn-doped ZnO film were performed under both zero-field-cooled (ZFC) and field-cooled (FC) conditions. The inset of Fig. 1 clearly shows an apparent deviation of ZFC and FC magnetizations up to the instrument limitation of 350 K, indicating that para- and diamagnetic contributions to the hysteresis loop can be eliminated.[4] Thus, we conclude that the magnetization hysteresis loops

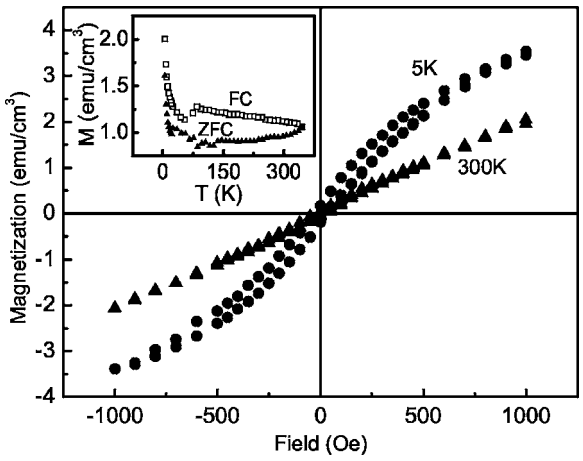

FIG. 1. Magnetization hysteresis curves of a $Zn_{1-x}Mn_xO$ (x=0.07) film at 5 and 300 K. The inset shows the FC and ZFC temperature-dependent magnetizations of $Zn_{1-x}Mn_xO$ (x=0.07).

can be attributed to the ferromagnetism of the Mn-doped ZnO film.

Figure 2 shows XRD 2θ scan spectra of the undoped ZnO and Mn-doped ZnO films, indicating that the films have c-axis oriented single-phase wurtzite structures. No extra diffraction peak from Mn-related second phases was observed. The XRD 2θ peak of $Zn_{1-x}Mn_xO$ (0002) is weak and broad, compared to that of undoped ZnO (0002). This suggests that Mn doping may cause some lattice disorder in the ZnO film although the wurtzite structure was maintained.

Figure 3 shows random and ⟨0001⟩ channeled RBS spectra of (a) the undoped ZnO and (b) the Mn-doped ZnO film. The Mn content in the Mn-doped ZnO film was estimated to be about 7% from a quantitative fit of the RBS measurement. The aligned yield (χ_{ZnO}) of about 5% from the undoped ZnO film [Fig. 3(a)] indicates good crystalline quality. The aligned yield from the Mn-doped ZnO film is about 60% [Fig. 3(b)], which indicates that a large amount of structural disorder might have been induced by the Mn incorporation, as shown by the broadening of the XRD 2θ diffraction peak for Mn-doped ZnO (Fig. 2). Further analysis using particle-induced x-ray emission (PIXE) and RBS in the channeling direction revealed that 25% of Mn substituted for Zn ions in

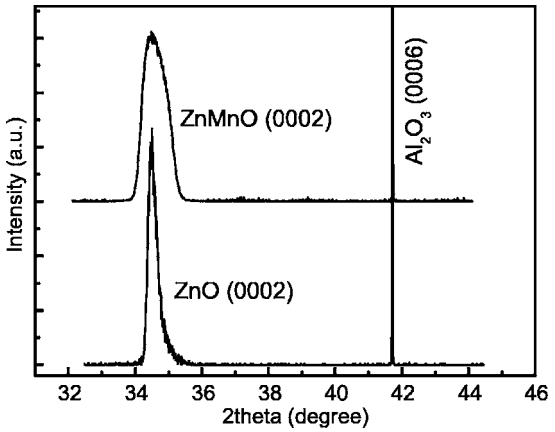

FIG. 2. XRD 2θ scan spectra of undoped ZnO and $Zn_{1-x}Mn_xO$ (x=0.07) films.

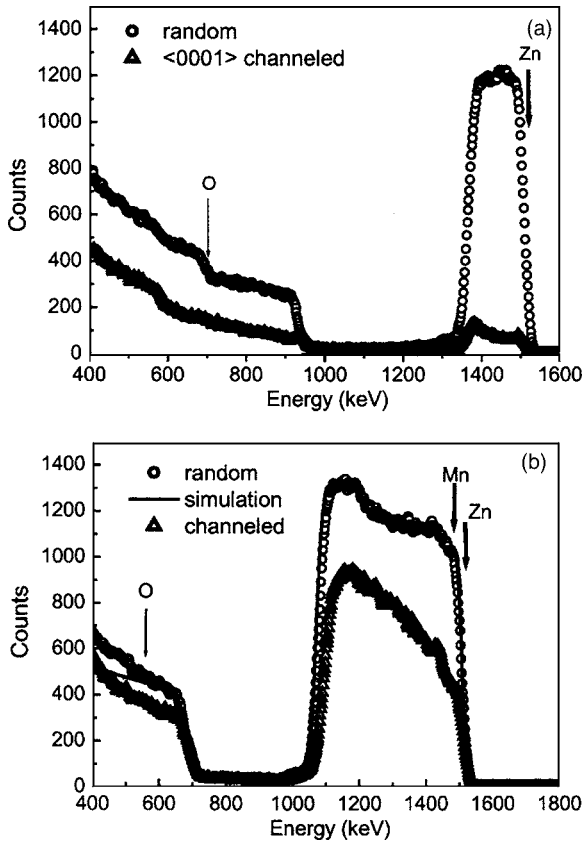

FIG. 3. Random and ⟨0001⟩ channeled RBS spectra of (a) 0.2-μm-thick undoped ZnO, and (b) 0.35-μm-thick Mn-doped ZnO film deposited on a 0.15-μm-thick undoped ZnO buffer layer.

the ZnO lattice forms wurtzite $Zn_{1-x}Mn_xO$, while most of the Mn incorporated in the ZnO film may be present in other forms.

A bright-field (BF) cross-sectional TEM image of the Mn-doped ZnO film is shown in Fig. 4(a). The interfacial layer between the sapphire and the undoped ZnO layer is comprised of an ~2.5-nm-thick polycrystalline layer. The crystallites are cubic with their (111) lattice planes parallel to the (0001) lattice planes of the hexagonal undoped ZnO layer. An energy dispersive x-ray spectroscopy (EDS) analysis indicates that this interface layer contains Mn, giving rise to a trimetallic phase of the type $(AlMn)ZnO_3$. It is not yet

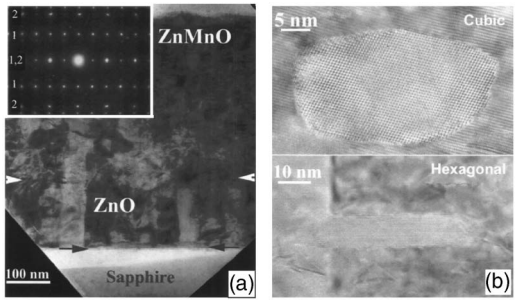

FIG. 4. (a) Bright-field cross-sectional TEM image of the Mn-doped ZnO thin film. The interfaces of undoped ZnO buffer/sapphire and Mn-doped ZnO/undoped ZnO buffer are indicated by the arrows. The inset is the selective-area electron-diffraction pattern from the undoped ZnO buffer layer. (b) Magnified cross-sectional TEM images of the cubic and hexagonal precipitates in the Mn-doped ZnO layer.

clear if this phase was formed during the deposition or the subsequent annealing, further work is in progress to elucidate this issue.

The columnar growth mode of the undoped ZnO buffer layer is shown in Fig. 4(a). The columns have an average domain size of about 50 nm. The contrast between columns in the undoped ZnO buffer layer is due to the 90° rotation misalignment of the $[11\bar{2}0]$ and $[1\bar{1}00]$ zone axes, which are parallel in the ZnO diffraction pattern as displayed in the inset of Fig. 4(a) for the selected crystallites. In the diffraction pattern, the spot lines labeled 1 and 2 belong to the $[11\bar{2}0]$ and $[1\bar{1}00]$ zone axes, respectively. When the Mn doping is initiated, the crystalline columns are disrupted and the Mn-doped ZnO layer contains a high density of precipitates, some of which appear as dark areas in Fig. 4(a). Figure 4(b) shows magnified cross-sectional TEM images of one of the round-shaped cubic and elongated hexagonal precipitates. Detailed analyses of the precipitates by EDS and lattice spacing measurement identified the round-shaped precipitates as the perovskite phase of $ZnMnO_3$ and the elongated hexagonal precipitates as $MnZn_3O_6$.

Concerning the observed room-temperature magnetization hysteresis of the Mn-doped ZnO film, the following considerations can be stated based on the structural analyses mentioned above. Firstly, the magnetic properties of Mn-related oxide precipitates, such as $ZnMnO_3$,[8] $(Mn,Zn)Mn_2O_4$,[9] and Mn_3O_4,[10] can be considered. It has been reported that $ZnMnO_3$ precipitates induce a spin-glass behavior in paramagnetic $Zn_{1-x}Mn_xO$ polycrystalline films, resulting in the merging of the ZFC and FC magnetization curves at the spin-freezing temperature (10–20 K).[8] However, the ZFC and FC magnetization curves of our Mn-doped ZnO film did not show the typical spin-glass behavior and merged at the instrument limit of 350 K (inset of Fig. 1). Further work will be needed to clarify the contribution of the observed cubic and hexagonal phase precipitates to the room-temperature hysteresis. The presence of Mn_3O_4 cannot explain the room-temperature hysteresis of Mn-doped ZnO film because of its low Curie temperature of 42 K,[10] and the $(Mn,Zn)Mn_2O_4$ was reported to be ferrimagnetic with Curie temperature less than 40 K.[9] The second consideration is on the small volume fraction of wurtzite $Zn_{1-x}Mn_xO$ in the Mn-doped ZnO film. The ferromagnetism of $Zn_{1-x}Mn_xO$ would be expected when the $Zn_{1-x}Mn_xO$ film is *p* type with a very high hole concentration.[2] However, in this study, no *p*-type dopant was introduced into the $Zn_{1-x}Mn_xO$ layer, and van der Pauw Hall measurements revealed that the Mn-doped ZnO film is semi-insulating. At this point, the origin of the observed ferromagnetism in the Mn-doped ZnO thin films cannot be clarified due to the unknown magnetic property of the observed precipitate $MnZn_3O_6$. However, it should be mentioned that when researchers interpret the origin of experimentally observed ferromagnetism in Mn-doped ZnO, the following should be considered: (1) the possible existence of the two precipitates reported in this article and (2) the actual substitutional Mn composition which could be much lower than the total Mn composition in the film.

In conclusion, we report on an investigation of the structural properties of ferromagnetic Mn-doped ZnO thin films deposited by rf magnetron sputtering. The substitutional fraction of Mn was about 25% in the Mn-doped ZnO film, indicating that most of the Mn incorporated in the film was present in other forms. TEM revealed that the incorporation of Mn led to a high density of round-shaped cubic and elongated hexagonal MnZn oxide precipitates in the crystalline columnar ZnO lattice. In addition, a trimetallic $(AlMn)ZnO_3$ phase was found in the ZnO/sapphire interface region.

This work was supported by AFOSR (Dr. T. Steiner) and ONR (Dr. C. E. C. Wood), and benefited from SBIR grant by MBO through Cermet Inc. (Dr. C. W. Litton).

[1] J. K. Furdyna, J. Appl. Phys. **64**, R29 (1988).
[2] T. Dietl, H. Ohno, F. Matsukura, J. Cibert, and D. Ferrant, Science **287**, 1019 (2000).
[3] S. W. Jung, S.-J. An, G.-C. Yi, C. U. Jung, S.-I. Lee, and S. Cho, Appl. Phys. Lett. **80**, 4561 (2002).
[4] D. P. Norton, S. J. Pearton, A. F. Hebard, N. Theodoropoulou, L. A. Boatner, and R. G. Wilson, Appl. Phys. Lett. **82**, 239 (2003).
[5] S. Lim, M. Jeong, M. Ham, and J. Myoung, Jpn. J. Appl. Phys., Part 2 **43**, L280 (2004).
[6] G. Lawes, A. S. Risbud, A. P. Ramirez, and R. Seshadri, Phys. Rev. B **71**, 045201 (2005).
[7] M. Venkatesan, C. B. Fitzgerald, J. G. Lunney, and J. M. D. Coey, Phys. Rev. Lett. **93**, 177206 (2004).
[8] S. Kolesnik, B. Dabrowski, and J. Mais, J. Supercond. **15**, 251 (2002).
[9] S.-J. Han, T.-H. Jang, Y. B. Kim, B.-G. Park, J.-H. Park, and Y. H. Jeong, Appl. Phys. Lett. **83**, 920 (2003).
[10] Y. M. Kim, M. Yoon, I.-W. Park, Y. J. Park, and J. H. Lyou, Solid State Commun. **129**, 175 (2004).